SIFIED

UNCLASSIFIED

[redacted]

CIC-14 REPORT COLLECTION

REPRODUCTION
COPY

110

[redacted]

C.3

[redacted]

SPECIAL RE-REVIEW
FINAL DETERMINATION
UNCLASSIFIED, DATE: 7/1/80

VERIFIED UNCLASSIFIED
LMR 6-11-79
JLW 7-1-80



[redacted]

UNCLASSIFIED

LA REPORT 110

[redacted]

July 21, 1944

This document contains 15 pages

# LEAD SPHERE INTEGRAL EXPERIMENT

WORK DONE BY:

W. Rarita

R. Serber

REPORT WRITTEN BY:

W. Rarita

R. Serber

## ABSTRACT

The set-up, the differential cross section data and the mathematical technique of the lead sphere integral experiment bear a close resemblance to their counterparts in a critical-mass or multiplication-rate calculation. The successful integration of the nuclear properties of lead, 25 and 28 in this problem gives us confidence in our ability to treat the more complex problem of the gadget. The agreement between theory and experiment is satisfactory. The ratio R (defined on pages 3 and10) for the two detectors 25 and 28 are compared in the table below:

| | $R_{exp}$ | $R_{theor}$ |
|---|---|---|
| 28 | 1.36 | 1.40 |
| 25 | 1.77 | 1.93 |

[redacted]

## LEAD SPHERE INTEGRAL EXPERIMENT

It is a long road from the measurement of differential nuclear properties to a detailed prediction of the behavior of neutrons in an actual gadget. The accumulation of numerous errors, both experimental and theoretical, might be feared to lead to large uncertainties in such a prediction. It is in this light that the lead sphere integral experiment is particularly interesting; the set-up itself, the differential data which must be used and the mathematical problem, all bear a close resemblance to their counterparts in a critical-mass or multiplication-rate calculation. For example, the nuclear properties which must be known include the fission spectrum, the transport and inelastic cross sections in the lead tamper, the spectrum of inelastically scattered neutrons, and the fission cross sections in 25 and 28. The successful integration of all these data in the case of the lead sphere experiment gives some feeling of confidence in our ability to treat the more complex problem of the gadget.

We shall briefly describe the experimental arrangement[1]. A thin spherical shell of 25 is bombarded with slow neutrons from a carbon pile. In the center of the 25 shell is placed a 25 or 28 fission detector (shielded by Cd and B). Immediately outside the 25 shell, the spherical lead tamper can be snugly fitted. Counts of neutron flux are made with and without the tamper in place. The ratio R of the two counts is then a measure of the reflection of the tamper.

1) Forthcoming report of DeWire, Wilson, and Woodward.

[redacted]

[redacted]

## Theory of the Experiment

Let us consider the Boltzmann transport equation for a steady state. The loss in neutron density (n) per second for a velocity $\underline{v}$ due to streaming and total scattering $(\sigma)$ out of the beam is compensated by the elastic $(\sigma_e)$ and inelastic $(\sigma_i)$ scattering and from the source S.

$$\underline{v}\cdot\nabla n = -\sigma v n + \int \sigma_e(\gamma)\, v' n(\theta')\,(d\Omega'/4\pi) + \int_E^\infty \chi_i(E,E')\,dE' \int \sigma_i' v' n(\theta')(d\Omega'/4\pi) + (S/4\pi) \qquad (1)$$

The primes label the neutron $(v', \theta')$ inelastically or elastically scattered to velocity v, θ. Also $\chi_0(E,E')$ is the probability of a neutron being inelastically scattered from energy E' to energy E. Introduce

$$n(\theta) = w_k(\theta)e^{ikr\cos\theta} \equiv w_k e^{ikr\mu};\quad n_k \equiv \int w_k\, d\Omega;\quad m_k \equiv \int w_k \cos\theta\, d\Omega;$$

$$S \equiv S_k\, e^{ikr\mu}$$

and let us suppose that

$$\sigma_e(\gamma) \equiv \sigma_e{}^0 + \sigma_e{}^{(1)}\cos\gamma$$

Then Eq. (1) becomes

$$ikv\mu\, w_k = -\sigma v w_k + v\,\sigma_e{}^0\,(n_k/4\pi) + \mu v\sigma_e{}^{(1)}(m_k/4\pi) + \int_E^\infty \chi_i\, dE'\sigma_i' v'(n_k'/4\pi) + (S_k/4\pi) \qquad (2)$$

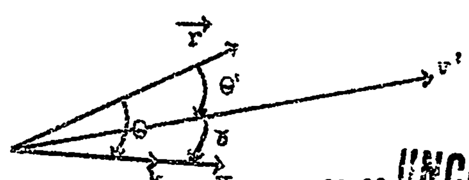


Fig.



[redacted]

We have assumed spherical scattering for the inelastic collisions. Rewriting Eq. (2)

$$v(\sigma + ik\mu)w_k = A + B\mu$$

$$A \equiv \left(v\,\sigma_e^{0}\, n_k + \int_E^{\infty} \chi_i\, \sigma_i'\, v'\, n_k'\, dE' + S_k\right)/4\pi \tag{3}$$

$$B \equiv v\,\sigma_e^{(1)}(m_k/4\pi)$$

$$n_k = \int w_k\, d\Omega = \frac{2\pi}{v}\int_{-1}^{+1} \frac{A + B\mu}{\sigma + ik\mu}\, d\mu$$

$$= \frac{2\pi}{v}\left\{\frac{A}{ik}\ln\frac{\sigma + ik}{\sigma - ik} + \frac{B}{(ik)^2}\left(2\,ik - \sigma \ln\frac{\sigma + ik}{\sigma - ik}\right)\right\} \tag{4}$$

$$m_k = \int w_k \cos\theta\, d\Omega = \frac{2\pi}{v}\int_{-1}^{+1} \frac{A\mu + B\mu^2}{\sigma + ik\mu}\, d\mu$$

$$= \frac{2\pi}{v}\left\{\frac{A}{(ik)^2}\left(2\,ik - \sigma\ln\frac{\sigma + ik}{\sigma - ik}\right) - \frac{B\sigma}{(ik)^3}\left(2\,ik - \sigma\ln\frac{\sigma + ik}{\sigma - ik}\right)\right\} \tag{5}$$

Solving for $n_k$ from these equations, we get

$$n_k = (2\pi/v)\, A\, (F_k/ik) \tag{6}$$

where

$$F_k = \ln\frac{\sigma + ik}{\sigma - ik} + \frac{1}{2}\,\frac{\sigma_e^{(1)}}{(ik)^3}\;\frac{\left(2\,ik - \sigma\ln\frac{\sigma + ik}{\sigma - ik}\right)^2}{\left[1 + \frac{1}{2}\frac{\sigma_e^{1}}{(ik)^3}\left(2\,ik - \sigma\ln\frac{\sigma + ik}{\sigma - ik}\right)\right]}$$

Transposing the first term on right and solving for $n_k v\sigma$,

$$n_k v\sigma = (S_k/G_k) + (1/G_k)\int_E^\infty \chi_i\, \sigma_i'\, v'\, n_k'\, dE' \quad \text{where} \tag{8}$$

$$G_k \equiv (2ik/F_k\sigma) - (\sigma_e{}^0/\sigma) \tag{8'}$$

By differentiating both sides of Eq. (8) with respect to E and integrating the resulting differential equation, we get

$$\begin{aligned} n_k v\sigma &= -\frac{1}{G_k}\int_E^\infty \frac{\partial S_k'}{\partial E'}\, e^{\int_E^{E'} \frac{\chi_i\,\sigma_i}{G_k\,\sigma}\, dE}\, dE' \\ &= \frac{S_k}{G_k} + \frac{1}{G_k}\int_E^\infty \frac{S_k'}{G_k'}\, \chi_i\, \frac{\sigma_i'}{\sigma'}\, e^{\int_E^{E'} \frac{\chi_i\,\sigma_i}{G_k\,\sigma}\, dE}\, dE' \end{aligned} \tag{9}$$

Eq. (8) may also be solved by iteration:

$$n_k v\sigma = \frac{S_k}{G_k} + \frac{1}{G_k}\int_E^\infty \chi_i\, (E,E')\, \frac{\sigma_i'}{\sigma'}\, \frac{S_k'}{G_k'}\, dE' + \dots\dots\dots\dots \tag{10}$$

The neutron flux given by Eq. (10) clearly separates into a first term coming directly from the source, a second term from single inelastic collisions, a third term from double inelastic collisions, etc.

A simpler and perhaps preferable expression for $G_k$ than that derived above is

[redacted]

$$G_k = \frac{2\,ik}{\sigma_t \ln \frac{\sigma_t + ik}{\sigma_t - ik}} - \frac{\sigma_e'}{\sigma_t} \;; \tag{11}$$

where $\sigma_t$ is the transport cross section. (This equation can be formally obtained from Eq. (8') by setting $\sigma_e^{(1)} = 0$ and changing $\sigma$ into $\sigma_t$.) Three reasons may be invoked: a) the actual elastic scattering is more complicated than the assumed $\sigma_e = \sigma_e^{\,0} + \sigma_e^{(1)} \cos\theta$; b) for small $k/\sigma$, the derived $G_k$ reduces to the form of Eq. (11); and c) for larger $k/\sigma$, the numerical work of Frankel and Nelson (cf. LA-53A) indicate that (11) and (8') agree quite well.

At the center of a spherical cavity the neutron flux reflected by a tamper ($a \leq r \leq b$) is

$$n(o)v = \int_a^b \left\{ \sigma_e\, n(r)v + \int_E^\infty \chi_i\,(E,E')\; \sigma_i'\; n'(r)v'\; dE' \right\} \frac{e^{-\sigma_t(r-a)}\, dr}{4\pi\, r^2} \tag{12}$$

Here again for non-spherical scattering the transport cross section replaces the total cross section.

We shall introduce an ortho-normal set of functions $n(k_j r)$ defined in the interval $a \leq r \leq b$. The form of $n(kr)$ assumed in the derivation of the Boltzmann equation was essentially $e^{-ikr\mu + i\delta}$. But the result for $n_k v\sigma$ does not depend on the direction of $\underline{k}$. The appropriate angle-independent spherical solution for $n(kr)$ becomes then

$$n(k_j r) = C_j\, \frac{\sin\,(k_j r + \delta)}{r} \tag{13}$$

[redacted]

[redacted]

The conditions to be imposed are three:

$$\text{(a) normalization, or } \int_a^b r^2\, n\,(k_j r)\, dr = 1$$

$$\text{(b) } \frac{dn(k_j r)}{dr} = 0 \text{ for } r = a \text{ and} \tag{14}$$

$$\text{(c) } n\,(k_j b_j') = 0 \text{ where } b_j' = b + \frac{.7104}{\sigma_t}\,\frac{\arctan(k_j/\sigma_t)}{(k_j/\sigma_t)}$$

Thus $b_j'$ is the extrapolated end-point.

Condition (b) can be proved to give the correct asymptotic phase of the solution far from the cavity by using the conservation theorem for a steady state: neutrons created inside the medium leak thru the outside surface:

$$4\pi\, r^2\, \sigma\, (\lambda - 1)\, \frac{dn}{dr}\bigg|_{r\,=\,b} + \sigma f \int_a^b n(kr)\, 4\pi\, r^2\, dr = 0$$

$$\text{and } 1 + f = \frac{k/\sigma}{\arctan k/\sigma} \equiv \lambda \tag{14'}$$

Substituting Eq. (13) in Eq. (15), we finally get

$$4\pi\, r^2 \left[\frac{\cos\,(kr + \delta)}{kr} - \frac{\sin\,(kr + \delta)}{(kr)^2}\right]\bigg|_{r\,=\,a} = 0 \tag{14''}$$

or equivalently

$$(dn/dr)_{r\,=\,a} = 0 \tag{14'''}$$

[redacted]

[redacted]

The $n(k_j r)$ given by Eq. (13) and (14) are not exact solutions of the Boltzmann equation for a finite medium, but differ from the exact solution by small terms which fall off exponentially from the boundaries. But since Eq. (12) depends on an average of the density over the whole region, the neglect of such edge corrections is not likely to be serious.

The allowable value of $k_j$ determined by (b) and (c) above are obtained from

$$k_j a \cot k_j (b'_j - a) = -1 \tag{15}$$

We now expand $n(r)v\sigma$ or

$$n(r)v\sigma = \sum_j n_{k_j} v\sigma \, n(k_j r) \tag{16}$$

The expression for $n_{k_j} v\sigma$ has already been given in Eq. (8),(9), or (10). The source function $S(r)$, an infinitely thin shell of total strength $Q$ and located at $r''$ is

$$S(r) = \frac{Q}{4\pi}\frac{\delta(r - r'')}{r^2} \text{ or } Q = \int_0^b S(r)\, d\underline{r} \tag{17}$$

Further

$$S(r) = \sum_j S_{k_j} n(k_j r) \text{ and } S_{k_j} = (Q/4\pi)\, n\,(k_j r'') \tag{18}$$

[redacted]

[redacted]

The basic Eq. (12) requires for its evaluation but a single numerical integration over r and a summation over j. The series is rapidly convergent. Three terms gave adequate accuracy.

The neutron $n_s(o)v$ flux which comes directly from the source is

$$n_s(o)v = (Q/4\pi r''^2) \tag{19}$$

The reflection coefficient $C_T$ for a single energy is then

$$C_T = \frac{n(o)v}{n_s(o)v} \tag{20}$$

We still have to average over the fission spectrum $(dQ/dE)$ of the source and over the cross section of the detector d (either 25 or 28) to evaluate the ratio of counts R with and without the tamper in place.

$$R = 1 + \frac{\int (dQ/dE)\ C_T\ \sigma(d)dE}{\int (dQ/dE)\ \sigma\ (d)\ dE} \tag{21}$$

Experimental and Theoretical Results

The lead tamper chosen by DeWire, Wilson, and Woodward for the experiment was 7" in outer, and 3" in inner radius. The 25 source was 1/4" thick and fitted tightly inside the lead.

The fission cross sections for 25 and 28 used in the calculation are shown in Fig. 2. The ratio of $\sigma(25)$ averaged over the fission spectrum to $\sigma(28)$ average over the same spectrum is used in correcting the "25" foil to pure 25. This value is theoretically computed to be 4.7. The experimental

[redacted]

value of 6.5 ± 20 percent is not considered very accurate as the foils used were not very thin. The fission spectrum adopted is reported by Staub in LAMS-75 and 95. The lead data were based on values given by Olum and Weisskopf (LAMS-105). The assumed inelastic spectrum, chosen to give a simple fit to Manley's biasing experiments (LA-51 and LA-57) is represented in Fig. 3 and Fig. 4.

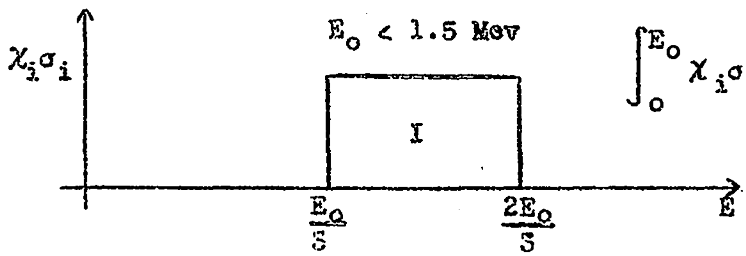


$$\int_0^{E_o} \chi_i \sigma_i \, dE = \sigma_i(E_o) = \sigma_i \ (I)$$

Fig. 3

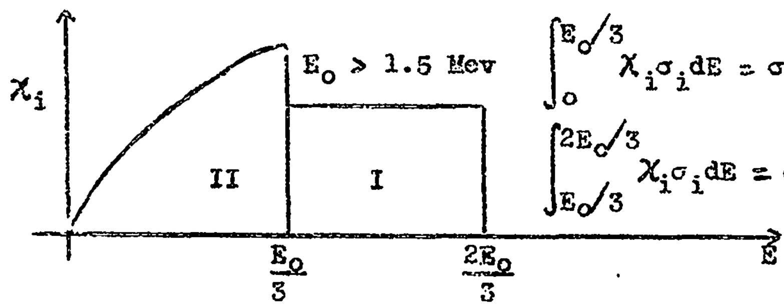


$$\int_0^{E_o/3} \chi_i \sigma_i \, dE = \sigma_i(II); \ \chi_i(E,E_o) \propto E^{\frac{1}{2}}; \int_0^{E_o/3} \chi_i \, dE = 1$$

$$\int_{E_o/3}^{2E_o/3} \chi_i \sigma_i \, dE = \sigma_i(I)$$

Fig. 4

The curves for $\sigma_i(I)$ and $\sigma_i(II)$ defined in Fig. 3 and Fig. 4 are given in Fig. 5.

It may be interesting to quote the results for $C_T$ the reflection coefficient for a single energy E. $C_T'$ is the same quantity neglecting inelastically degraded neutrons. These values are plotted in Fig. 6.

Finally, the theoretical and experimental values of the ratio R (see Eq. 18) for detectors 28 and 25 are listed in Table I. R' the value when inelastically degraded neutrons are neglected as first entered.

[redacted]

TABLE I

| | $R_{exp}$ | $R_{theor}$ | $R'$ |
|---|---|---|---|
| 28 | 1.36 | 1.40 | 1.32 |
| 25 | 1.77 | 1.93 | 1.64 |

The agreement is satisfactory although the numbers seem to indicate that the inelastic contribution has been somewhat overestimated.

[redacted]

[redacted]

Fig. 2

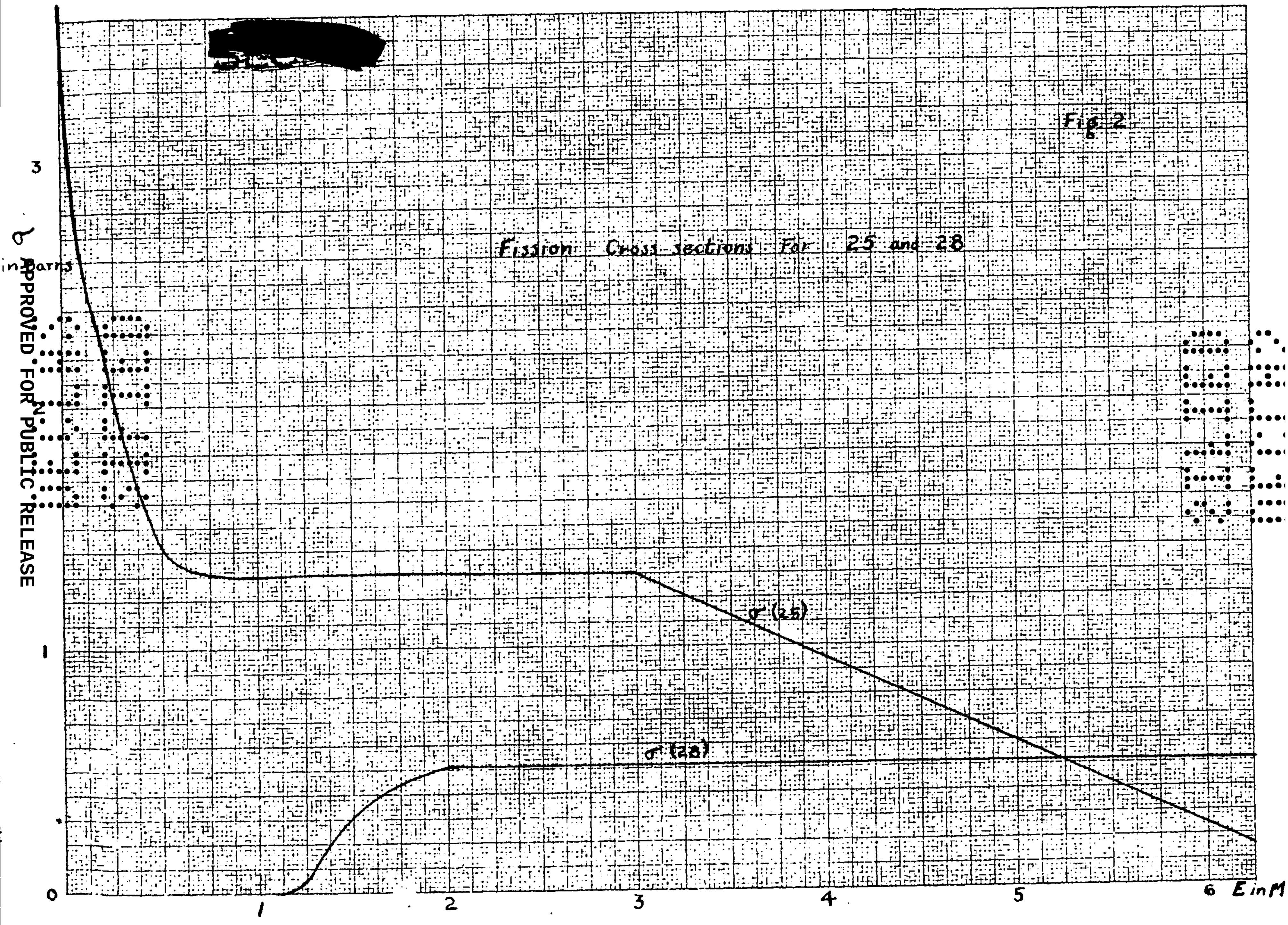



APPROVED FOR PUBLIC RELEASE

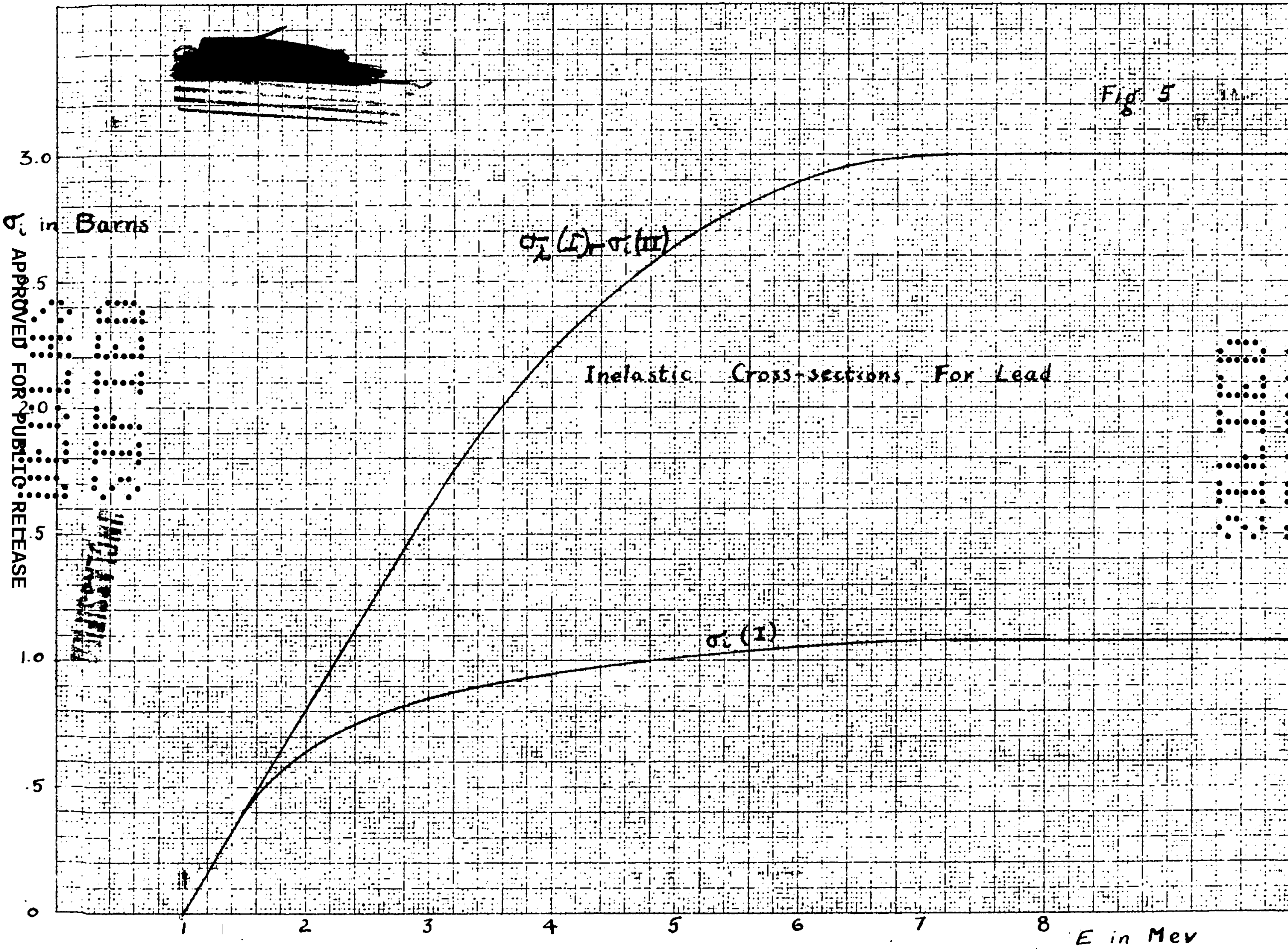
[redacted]
Fig. 5
Inelastic Cross-sections For Lead
$\sigma_i$ in Barns
$\sigma_i(I) + \sigma_i(III)$
$\sigma_i(I)$
3.0
2.5
2.0
1.5
1.0
.5
0
1
2
3
4
5
6
7
8
E in Mev

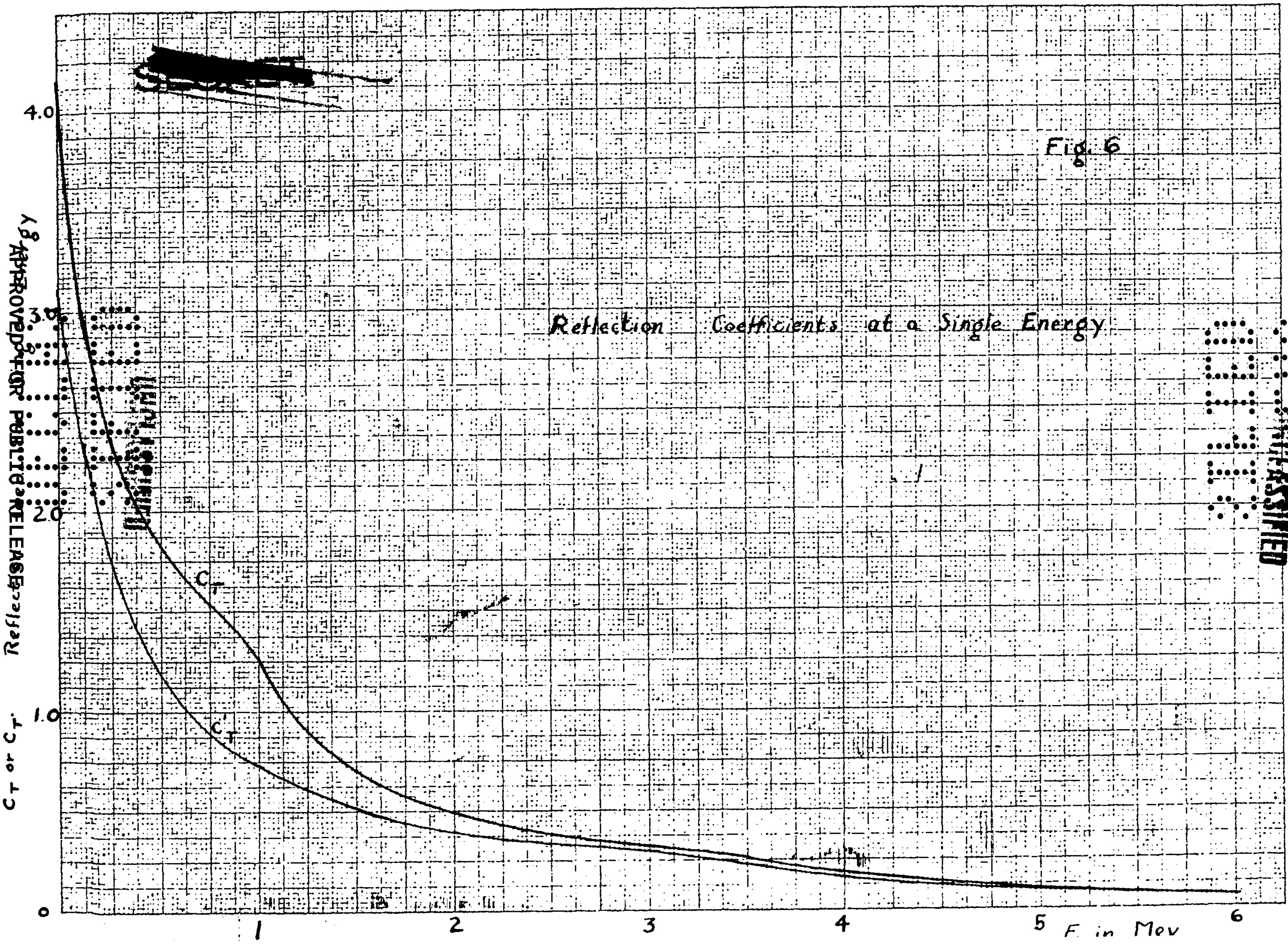
Fig. 6
Reflection Coefficients at a Single Energy
$C_T$
$C'_T$
$C_T$ or $C_T'$ Reflection Coefficients
4.0
3.0
2.0
1.0
0
1
2
3
4
5
6
E in Mev

DOCUMENT ROOM

REC. FROM ..15........

DATE.......7/22/50...

REC...........NO. REC.✓......